HHS Public Access

Author manuscript

Circ Cardiovasc Imaging. Author manuscript; available in PMC 2018 June 01.

Published in final edited form as:

Circ Cardiovasc Imaging. 2017 June ; 10(6): . doi:10.1161/CIRCIMAGING.117.005446.

Low Field Cardiac MRI: A Compelling Case for CMR's Future

Orlando P. Simonetti, Ph.D.[1,2,3] and **Rizwan Ahmad, Ph.D.**[3,4]

[1]Department of Internal Medicine, Division of Cardiovascular Medicine, The Ohio State University, Columbus, Ohio

[2]Department of Radiology, The Ohio State University, Columbus Ohio

[3]Dorothy M. Davis Heart and Lung Research Institute, The Ohio State University, Columbus, Ohio

[4]Department of Electrical and Computer Engineering, The Ohio State University, Columbus, Ohio

Introduction

Cardiac Magnetic Resonance (CMR) is arguably unmatched in its ability to evaluate cardiovascular structure and function, to characterize myocardial tissue by a wide variety of mechanisms, and to quantitatively assess blood flow and perfusion without the use of radiation or the need for invasive catheterization. CMR research and development continues at a rapid pace both in academia and by commercial vendors, and every year new techniques are put forth that improve on existing applications and provide new capabilities that further expand the clinical utility of this powerful modality. Real-time and single-shot techniques have made CMR feasible in patients with rhythm irregularities and inability to breath-hold. Ongoing development and regulatory approval of MRI conditional pacemakers and implanted cardioverter defibrillators continues to grow the patient population amenable to CMR. Larger clinical trials are coming out that support the clinical value of CMR[1–3]. Despite the advances in CMR technology over the past decades, the growing data supporting its effectiveness, and the increasing availability of both CMR-capable scanners and practitioners, the penetration of CMR into routine diagnostic cardiovascular imaging remains limited. It is clear that those involved in CMR research must not only engage in developing new and exciting applications made feasible by technological advances, but must also ask whether their technology will promote the routine clinical utilization of CMR beyond academic and isolated private centers. There are many factors at play in answering this question, but important considerations must be affordability and ease of use.

A CMR system is one of the most expensive devices in the hospital, and the cost of the system scales with field strength. Prior to 2001 the highest field strength available for clinical MRI was 1.5T; however, recent years have witnessed an expanded utilization of 3T MRI that has been driven mainly by neuro and orthopedic imaging and the desire for higher

Correspondence to Orlando P. Simonetti, PhD, Biomedical Research Tower Room 320, 460 W. 12th Ave., Columbus, OH 43210. Simonetti.9@osu.edu.

Disclosures

Free access to the 0.35T MRIdian system used to generate the images in this article was provided under a research agreement with Viewray, Inc.

spatial resolution that is critical for these applications. While just a few years ago it appeared that 3T would be “the new 1.5T,” the early excitement over promises of increased speed and image quality have been tempered as the reality of the additional practical challenges of ultra-high field CMR have set in, making it difficult to justify the increased cost over 1.5T. While increased field strength clearly provides the advantage of higher signal-to-noise [4], it also carries the baggage of a number of practical limitations [4–11], including increased magnet size and weight, increased potential for heating of implanted devices, increased ferromagnetic attraction, increased inhomogeneity in both the static field and the applied radiofrequency (RF) field, increased ECG interference, and increased image artifacts around metallic devices. In the present healthcare environment where cost-effectiveness has to be one of the primary considerations in resource utilization, healthcare providers may be more often asked to utilize more economical approaches rather than taking what may be the easier route of applying the most expensive solution to a problem or a clinical question. While MRI technology continues to move in the direction of higher field strength as evidenced by the proliferation of whole body 7T systems in academic centers, perhaps it is time to consider whether we can do “more with less,” especially in the context of CMR which has struggled to gain a foothold as a routine cardiovascular diagnostic tool.

The early days of whole-body MRI began with the use of much lower field systems, in the range of 0.15T to 0.35T. The use of lower magnetic field strength magnets may be worth revisiting in the interest of not only cost-savings, but also patient safety and ease of use. The prospect for excellent field homogeneity, in absolute terms, and virtually no limits imposed by Specific Absorption Rate (SAR) may open up the potential for new applications of techniques such as balanced steady state free precession (bSSFP), echo planar imaging (EPI), and spiral imaging that can be problematic at higher field strength. Early MRI systems based on permanent or resistive magnets did not have the benefits of high performance gradient systems or large banks of receiver channels. In contrast, the specifications of modern low-field systems compare more favorably to state-of-the-art high field systems. For example, the Panorama HFO 1.0T (Philips Healthcare, Amsterdam, Netherlands) is an open configuration system that employs an 8-channel RF receiver array and a gradient system with maximum amplitude of 28 mT/m and maximum slew rate of 120 mT/m. Another modern low-field system with gradient and RF performance comparable to high field scanners is a split-bore 0.35T MRI-guided radiation therapy system (MRIdian, Viewray, Oakwood Village, OH) that is equipped with a gradient system with maximum amplitude of 18 mT/m and maximum slew rate of 200 mT/m/msec, and a 12-channel RF receiver system [12, 13]. The Viewray system has a 70 cm bore and claims field homogeneity of approximately 3 ppm over a 50 cm diameter sensitivity volume (DSV), which in absolute terms is equivalent to an approximate frequency offset of 45 Hz. Increasing maximum gradient amplitude and slew rate (rate of change of gradient) positively impacts the image quality and acquisition efficiency; increasing number of channels positively impacts the signal-to-noise ratio (SNR); and improving field homogeneity reduces artifacts. Most modern 1.5T systems have maximum gradient amplitudes of 20 to 45 mT/m, maximum slew rate of 100–200 mT/m/msec, a number of RF channels that ranges from 8 to 32, and field homogeneity of approximately 1.5–3 ppm over a 50 cm DSV. The specifications of the Viewray system, which is specially designed and marketed for real-time MRI guidance of

radiation therapy, are comparable to a modern 1.5T system. Therefore, this system provides an opportunity to explore the potential of low field CMR and was used to generate all of the 0.35T results shown here.

In this article, we will buck the current trend that anticipates a future for CMR that relies on the promise of higher field strength to enable new and potentially useful applications. Instead, we explore the possible advantages of lower field strength systems, below 1.5T, and the potential of a future that offers high quality, routine clinical CMR that is lower in cost, easier to perform, and safer for the growing population of patients with implanted devices. We examine and explain the specific disadvantages of ultra-high field for CMR and explore the potential advantages, beyond cost, that argue in favor of considering low field as the future of CMR.

The technical aspects of CMR at low field

The choice of optimal CMR scan parameters involves compromises between SNR, temporal resolution, spatial resolution, scan time, and artifact level. In simplistic but practical terms, SNR scales linearly with magnetic field strength, and SNR is essentially the “currency” in MRI that can be traded for acquisition speed and spatial resolution. This has been the main driving force behind the move towards 3T and higher field strength systems. With greater field strength also comes greater spectral separation, which is useful in spectroscopy and for some fat suppression techniques, although the advantage in spectral separation may be offset by increased field inhomogeneity, which also scales with field strength. Finally, T1 increases with field strength, and this can be advantageous in contrast-enhanced imaging as the differential between enhanced and unenhanced tissue may be greater. Of course, increased T1 may also be disadvantageous depending on the technique as it can reduce SNR if not compensated by using longer repetition times (TR) or lower flip angle. While the primary advantage of higher field thus is higher SNR, there are a number of disadvantages as well and many of these are directly relevant to CMR. Significant research and development efforts have gone into overcoming these limitations and disadvantages in order to make CMR performance acceptable at 3T. In contrast, at low field many of the factors that limit CMR at higher field are reduced, or in some cases nonexistent, and the only real question is whether sufficient SNR can be generated for high quality diagnostic imaging. In the next sections we look at some of the many factors related to CMR image quality and safety, and how they are influenced by field strength.

Signal-to-Noise Ratio (SNR)

The theoretically linear relationship between SNR and field strength has been shown to bear out in practice, with the caveat that the expected gains at higher field can be limited by increased native T1 and limitations on flip angle set by increased patient Specific Absorption Rate (SAR)[6, 7]. However, it should first be considered whether the SNR available at lower field may be sufficient to generate diagnostic quality CMR images [14], especially when bSSFP based pulse sequences and compressed sensing (CS) inspired image recovery methods are employed. Figure 1 shows the degradation in the quality of a segmented bSSFP cine series acquired at 1.5T when the SNR is retrospectively reduced by adding noise to the

measured k-space data to simulate the impact of reduced field strength on SNR alone. As evident from the results, sufficient image quality is maintained even when the SNR is degraded to levels expected at field strengths of 0.5T or less. In this simulation, only the negative impact of reduced SNR is considered; the potential advantages of higher homogeneity, shorter T1, and reduced SAR allowing higher flip angles are not demonstrated.

Figures 2, 3 and 4 show the feasibility of three basic CMR applications: bSSFP cine (Figure 2), spoiled gradient echo phase-contrast MRI (Figure 3), and black blood turbo spin echo (Figure 4), at low field. For all three results, fully sampled datasets were collected from healthy volunteers on a 0.35T scanner. The k-space data were then retrospectively down-sampled by a factor of two in a pseudorandom fashion using the VISTA sampling technique [15] and reconstructed using a recently proposed compressed sensing (CS) method called Sparsity adaptive COmpressive REcovery (SCoRe)[16]. For all three applications, the SNR at 0.35T appears adequate to generate diagnostic quality images, in this case even with data under-sampling. While anecdotal, these encouraging results demonstrate that high quality CMR can potentially be performed at low field even with scan parameters that would be typical at 1.5T or higher. The only modification to pulse sequence parameters in this case was to use a high flip angle of 110° for bSSFP cine. While a flip angle this high may provide optimal blood-myocardium CNR [17], it would not normally be feasible at 1.5T or above due to SAR limitations. One could expect further improvement in the image quality by additional optimization of imaging parameters specifically for low field. Furthermore, the receiver coil on this system is designed for large field-of-view thoracic and abdominal imaging, and also specifically designed to not interfere with the radiation therapy. Additional gains in cardiac imaging performance may be expected with a receiver coil optimized for CMR.

Safety

SAR—A number of patient safety factors are related to field strength, and in nearly every case the concerns are greater at higher field. SAR scales as the square of field strength; thus for equivalent pulse sequences utilizing the same RF pulses, SAR would be 9 times higher at 1.5T than at 0.5T, and 36 times higher at 3T than at 0.5T. SAR is carefully monitored in real-time on clinical MRI systems so as not to exceed the FDA limit of 4 W/kg (whole body SAR). Pulse sequence parameters are automatically modified by scanner software to keep the SAR within FDA limits for each scan. Thus, except in patients unable to thermo-regulate or when scanning patients with implanted devices, the safety risks related to SAR have been mitigated, but it still represents a limiting factor in image quality. For example, the flip angle for optimal blood-myocardium contrast to noise ratio (CNR) in bSSFP cine has been shown to be in the range of 105° [17], yet at 3T flip angles may be restricted by SAR limits to 50° or lower, significantly curtailing any theoretical gains in CNR potentially afforded by higher field strength. As shown in Figure 2, at 0.35T the SAR limits are not a factor and high flip angles can be used to maximize CNR.

Device heating—The Larmor frequency, and thus the transmitted RF frequency, is directly proportional to field strength; thus the RF frequency at 3T (128 MHz) is twice that

at 1.5T (64 MHZ), and six times that at 0.5T (21 MHz). This has implications for the heating of any implanted device that is made of conductive materials. Although most modern devices do not pose any significant heating risk at 1.5T, the potential for heating of devices of sizes that can be implanted in the human body is even further reduced at lower field. For example, at 3T the resonant half-wavelength (indicative of the length of device likely to demonstrate RF-induced heating) is 13 cm, and at 1.5T it is 26 cm, while at 0.5T it is approximately 78 cm. While gradient switching and RF pulsing must also be considered in the compatibility of active implants such as pacemakers and defibrillators, overall the safety of patients with implants would only improve at lower field [18] with reduced risk of device heating. The risks associated with ferromagnetic attraction of external devices and instruments are also reduced with lower field systems, as are the level of artifacts surrounding metallic implants [19].

Physics advantages of low field

While the loss of SNR at low field considered in isolation is clearly a disadvantage, there are numerous other physical factors at play that may adequately compensate for the lost SNR. Given the preponderance of CMR techniques that are, or can be, based on the bSSFP readout including cine, perfusion, late gadolinium enhancement (LGE), T1 mapping, T2 mapping, and non-contrast angiography, it is possible that much of the SNR lost at lower field may be gained back by appropriate choice of pulse sequence and imaging parameters. bSSFP is the most efficient acquisition strategy in terms of SNR per unit time, and its effectiveness at low field is well-known [20, 21]. Besides SAR limiting the effectiveness of bSSFP at 3T and above, especially for cine and bright blood angiography, the technique is also highly sensitive to static magnetic field homogeneity. In absolute terms, inhomogeneity scales directly with field strength; e.g., 2 ppm homogeneity at 3T implies a 255 Hz offset in the proton resonant frequency, while at 0.5T the same 2ppm homogeneity represents only a 42 Hz frequency offset. Subject (patient) induced inhomogeneities around the heart, particularly at the heart-liver-lung interface, can easily be as high as 2 ppm [22, 23], and of course susceptibility gradients are much worse around implanted metallic devices such as stents, sternal wires, or orthopedic devices[19]. The implications of improved field homogeneity at lower field could be dramatic in terms of the applicability of bSSFP across a variety of scan techniques, and potentially would open the door to routine utilization of bSSFP at low field for applications such as LGE and first-pass perfusion. At higher field strengths, bSSFP is often avoided for applications where myocardial signal intensity is of interest, as is the case for LGE and first-pass perfusion, because of the characteristic dark-band artifacts [24] that can result even with careful shimming at high field. The air in the lungs and airways can cause steep susceptibility gradients around the heart [22, 23] that are difficult to compensate even with patient-specific shimming procedures. The sensitivity to field homogeneity of bSSFP is related to the TR; the shorter the TR the less sensitive it is to banding artifacts [25]. Thus at high field, high receiver bandwidth and reduced spatial resolution are commonly used to keep TR as short as possible [26]. While these sequence modifications may reduce artifact, they also offset the potential SNR and resolution advantages one would hope to gain with higher field. With greater field homogeneity at low field, longer TR is possible and thus SNR can be improved by reducing receiver bandwidth lower than typically feasible at 3T. In Figure 5, for example, bSSFP cine images were

acquired at 0.35T and 1.5T with low receiver bandwidth resulting in a relatively long TR 9.3 ms. No specific patient shimming was applied in either case. Note the dramatic difference in the level of artifact between the two systems, illustrating the point that reduced receiver bandwidth may be feasible at low field to help compensate for the inherent loss of SNR.

Beyond bSSFP, improved field homogeneity and reduction in susceptibility gradients would also provide advantages for techniques utilizing EPI and spiral readouts, allowing access to the efficiency gains afforded by these techniques that are not easily applied at higher field. Factors such as these illustrate that any investigation of CMR at low field must be undertaken with an open realization that the optimal approaches to image acquisition may turn out to be very different than the methods that are routinely used at 1.5T and above.

Implications of model based image reconstruction methods

In the last ten years, significant strides have been made in the field of model based image recovery [27], where the image reconstruction relies not only on the data, but also utilizes the rich spatial and temporal structure inherent in the images. For example, compressed sensing, which is a particular flavor of model based processing, has enabled MRI recovery from highly under-sampled data [28, 29]. CS-based methods have been highly effective for CMR applications due to the inherent spatial and temporal redundancies in dynamic imaging, resulting in acceleration rates of eight or more [15, 30]. However, the current application of CS to CMR has been narrowly focused on recovering images from highly under-sampled, high-SNR data, primarily to accelerate scan times. By drawing equivalence between a small number of high-SNR samples and a large number of low-SNR samples, it can be argued that CS-based methods would be effective for low-field application as well. At low-field, CS may not enable acceleration rates in excess of 8, but attaining moderate acceleration rates of two or three is very likely to be within reach. Such moderate acceleration rates are what can be typically achieved using parallel MRI techniques at high field and have been proven adequate for routine CMR applications.

One can argue that CS reconstruction is even better suited for low field than high field. Although higher SNR is available at high-field, stronger field inhomogeneity at high-field can cause data corruption, leading to structured artifacts and model mismatch. It has been well-established that model based imaging techniques, including CS, are effective in handling noise or noise-like artifacts but are not well-equipped to handle structured artifacts and model mismatch. Therefore, one can expect low-field CMR, which is primarily limited by SNR and less so by field inhomogeneity related artifacts, is a better candidate to benefit from CS. Figure 5 provides an example, where a CS-based method, SCoRe, does not benefit the reconstruction of 1.5T cine data with long TR and significant inhomogeneity artifacts. In fact, SCoRe seems to make artifacts worse due to the model mismatch, while at low field the reduced SNR leads to a higher relative level of random background noise, which is more easily suppressed by CS methods. Thus, the use of CS reconstruction techniques in the realm of reduced SNR data may shift things in favor of low field CMR in a way that would not have been feasible just a few years ago.

Cost advantages of low field

An MRI machine is clearly one of the most expensive pieces of equipment utilized for cardiovascular diagnostic imaging. A 1.5T system fully outfitted for CMR can easily cost $1.25M, and a state-of-the-art 3T system may cost upwards of $2.0M. Add to that an additional $0.75M to $1.0M for site preparation and construction and the total costs for a 3T can easily exceed $2.5M. Meanwhile, there is significant downward pressure on the reimbursement for CMR as well as for many other diagnostic imaging procedures. Recently, in fact, the US Centers for Medicare and Medicaid Services (CMS) reduced reimbursement for outpatient stress perfusion CMR by over 40%. CMR can only survive in this environment by continuing to generate data demonstrating its high diagnostic and prognostic value, and by taking measures to reduce cost wherever possible. Without any concrete demonstration of clear advantages for high-field CMR, pushing to 3T and higher along with the necessarily greater purchase and siting expenses certainly goes against the critical need to reduce cost. While it is challenging to accurately project the price of a lower field (0.35T to 1.0T) MRI system with high performance gradient and RF subsystems, a lower field magnet is inevitably less expensive, and there would potentially be additional savings in terms of lower frequency electronics, reduced siting costs with a lighter magnet, and perhaps less shielding. If adequate diagnostic quality could be provided for the basic CMR applications (cine, perfusion, LGE, flow, angiography) at a significantly reduced equipment cost, it would only favor the broader utilization of CMR in the future. This again argues in favor of the exploration of low field CMR rather than solely focusing research and development efforts on higher field, more expensive MRI machines.

Ease of use

Along with the high cost, the complexity of CMR represents another significant reason that the modality has not been more widely adopted. The large number of available techniques from which to choose and scan parameters to set can be confusing to the novice, scan planes must be adapted to complex anatomy, and artifacts can be difficult to recognize and compensate. Performing CMR at 3T and above only adds to the complexity. Additional patient-specific shimming is often required [31]; obtaining a reliable electrocardiogram (ECG) signal is more challenging [32]; special frequency adjustments may be needed to avoid severe artifacts in bSSFP cine images [33]; artifacts surrounding metallic implants such as stents and sternal wires can be far reaching [19]; and RF inhomogeneities can cause signal variations across the image [6] that are non-existent at lower field strengths. Additional troubleshooting may be required by the imager to modify pulse sequence parameters, or to change pulse sequence types entirely when artifacts are encountered. Some techniques that are routine at 1.5T, such as bSSFP cine, can fail due to excessive artifacts in some patients scanned at 3T. All of these factors contribute to the fact that higher field strength leads to greater complexity in scanning. If the imager is not totally familiar with the causes and solutions to a wide range of artifacts that only manifest at higher field, they may spend significant additional time and effort trying to generate a level of image quality that is routine at 1.5T. All of these same issues, i.e., shimming, ECG, bSSFP artifacts, and RF inhomogeneity, would be even less problematic at lower field.

Another advantage of the low-field paradigm is the potential for system designs that are more patient friendly. Modern high-field systems exclusively use the solenoidal magnet design with little margin to alter the configuration or even the bore size. In contrast, the configuration of low-field systems should be easier to modify due to smaller magnet design and less stringent requirements for relative field homogeneity. Low-field magnets can be configured as “open” MRI systems, circumventing the issue of claustrophobia, improving patient monitoring, and increasing the opportunity to combine exercise stress testing and interventional procedures with CMR.

The future

Today when one thinks of a high tech automobile, an all-electric vehicle may be considered, or perhaps a car that is so automated it requires no operator at all. In the past, the focus might have been entirely on horsepower, while today it is more about fuel efficiency and ease of use. The same considerations should apply to CMR. While those involved in developing new CMR technology have always focused on increasing the speed of acquisition and image quality, these can no longer be goals to be achieved at all costs. CMR is not clinically underutilized because the quality of images and results are inadequate, or because the images cannot be acquired fast enough, but rather because it is expensive and can be difficult to use. Why not focus our research efforts on these aspects that are limiting broader utilization of CMR by exploring what can be done at low field with the same enthusiasm and resources that have been applied to high field CMR? There may be a surprising future for CMR at low field.

Supplementary Material

Refer to Web version on PubMed Central for supplementary material.

Acknowledgments

We thank Michael Hansen, Peng Hu, Krishna Nayak, Gerhard Laub, and Oliver Heid for helpful discussion, and James Dempsey, Bela Vajko, Georgi Gerganov, and Iwan Kawrakow of Viewray for access to and assistance with the MRIdian system.

Sources of funding

The authors are supported by research grants R21EB022277, R21EB021655, and R21EB021638 from the National Institute of Biomedical Imaging and Bioengineering.

References

1. Greenwood JP, Herzog BA, Brown JM, Everett CC, Nixon J, Bijsterveld P, Maredia N, Motwani M, Dickinson CJ, Ball SG, Plein S. Prognostic Value of Cardiovascular Magnetic Resonance and Single-Photon Emission Computed Tomography in Suspected Coronary Heart Disease: Long-Term Follow-up of a Prospective, Diagnostic Accuracy Cohort Study. Annals of internal medicine. 2016; doi: 10.7326/M15-1801
2. Greenwood JP, Maredia N, Younger JF, Brown JM, Nixon J, Everett CC, Bijsterveld P, Ridgway JP, Radjenovic A, Dickinson CJ, Ball SG, Plein S. Cardiovascular magnetic resonance and single-photon emission computed tomography for diagnosis of coronary heart disease (CE-MARC): a prospective trial. Lancet. 2012; 379:453–60. [PubMed: 22196944]

3. Schwitter J, Wacker CM, Wilke N, Al-Saadi N, Sauer E, Huettle K, Schonberg SO, Debl K, Strohm O, Ahlstrom H, Dill T, Hoebel N, Simor T. investigators M-I. Superior diagnostic performance of perfusion-cardiovascular magnetic resonance versus SPECT to detect coronary artery disease: The secondary endpoints of the multicenter multivendor MR-IMPACT II (Magnetic Resonance Imaging for Myocardial Perfusion Assessment in Coronary Artery Disease Trial). Journal of cardiovascular magnetic resonance : official journal of the Society for Cardiovascular Magnetic Resonance. 2012; 14:61. [PubMed: 22938651]
4. Wen H, Denison TJ, Singerman RW, Balaban RS. The intrinsic signal-to-noise ratio in human cardiac imaging at 1.5, 3, and 4 T. Journal of magnetic resonance. 1997; 125:65–71. [PubMed: 9245361]
5. Nael K, Fenchel M, Saleh R, Finn JP. Cardiac MR imaging: new advances and role of 3T. Magnetic resonance imaging clinics of North America. 2007; 15:291–300. v. [PubMed: 17893050]
6. Oshinski JN, Delfino JG, Sharma P, Gharib AM, Pettigrew RI. Cardiovascular magnetic resonance at 3.0 T: current state of the art. Journal of cardiovascular magnetic resonance : official journal of the Society for Cardiovascular Magnetic Resonance. 2010; 12:55. [PubMed: 20929538]
7. Rajiah P, Bolen MA. Cardiovascular MR imaging at 3 T: opportunities, challenges, and solutions. Radiographics : a review publication of the Radiological Society of North America, Inc. 2014; 34:1612–35.
8. Stanisz GJ, Odrobina EE, Pun J, Escaravage M, Graham SJ, Bronskill MJ, Henkelman RM. T1, T2 relaxation and magnetization transfer in tissue at 3T. Magnetic resonance in medicine. 2005; 54:5.
9. Dietrich O, Reiser MF, Schoenberg SO. Artifacts in 3-T MRI: physical background and reduction strategies. European journal of radiology. 2008; 65:29–35. [PubMed: 18162353]
10. Graf H, Lauer UA, Berger A, Schick F. RF artifacts caused by metallic implants or instruments which get more prominent at 3 T: an in vitro study. Magnetic resonance imaging. 2005; 23:493–9. [PubMed: 15862651]
11. Lauer UA, Graf H, Berger A, Claussen CD, Schick F. Radio frequency versus susceptibility effects of small conductive implants--a systematic MRI study on aneurysm clips at 1.5 and 3 T. Magnetic resonance imaging. 2005; 23:563–9. [PubMed: 15919602]
12. Mutic S, Dempsey JF. The ViewRay system: magnetic resonance-guided and controlled radiotherapy. Seminars in radiation oncology. 2014; 24:196–9. [PubMed: 24931092]
13. Saenz DL, Yan Y, Christensen N, Henzler MA, Forrest LJ, Bayouth JE, Paliwal BR. Characterization of a 0.35T MR system for phantom image quality stability and in vivo assessment of motion quantification. Journal of applied clinical medical physics. 2015; 16:5353.
14. Klein HM, Meyners W, Neeb B, Labenz J, Truummler KH. Cardiac magnetic resonance imaging using an open 0.35 T system. Journal of computer assisted tomography. 2007; 31:430–4. [PubMed: 17538291]
15. Ahmad R, Xue H, Giri S, Ding Y, Craft J, Simonetti OP. Variable density incoherent spatiotemporal acquisition (VISTA) for highly accelerated cardiac MRI. Magnetic resonance in medicine. 2015; 74:1266–78. [PubMed: 25385540]
16. Ahmad R, Schniter P. Interatively reweighted l1 approaches to sparse composite regularization. IEEE transactions on computational imaging. 2015; 1:16.
17. Srinivasan S, Ennis DB. Optimal flip angle for high contrast balanced SSFP cardiac cine imaging. Magnetic resonance in medicine. 2015; 73:1095–103. [PubMed: 24700652]
18. Strach K, Naehle CP, Muhlsteffen A, Hinz M, Bernstein A, Thomas D, Linhart M, Meyer C, Bitaraf S, Schild H, Sommer T. Low-field magnetic resonance imaging: increased safety for pacemaker patients? Europace : European pacing, arrhythmias, and cardiac electrophysiology : journal of the working groups on cardiac pacing, arrhythmias, and cardiac cellular electrophysiology of the European Society of Cardiology. 2010; 12:952–60.
19. Khan SN, Rapacchi S, Levi DS, Finn JP. Pediatric cardiovascular interventional devices: effect on CMR images at 1.5 and 3 Tesla. Journal of cardiovascular magnetic resonance : official journal of the Society for Cardiovascular Magnetic Resonance. 2013; 15:14. [PubMed: 23343398]
20. Duerk JL, Lewin JS, Wendt M, Petersilge C. Remember true FISP? A high SNR, near 1-second imaging method for T2-like contrast in interventional MRI at .2 T. Journal of magnetic resonance imaging : JMRI. 1998; 8:203–8. [PubMed: 9500281]

21. Sarracanie M, LaPierre CD, Salameh N, Waddington DE, Witzel T, Rosen MS. Low-Cost High-Performance MRI. Scientific reports. 2015; 5:15177. [PubMed: 26469756]
22. Atalay MK, Poncelet B, Kantor HL, Brady TJ, Weisskoff RM. Cardiac susceptibility artifacts arising from the heart-lung interface. Magnetic resonance in medicine. 2001; 45:5.
23. Reeder SB, Faranesh AZ, Boxerman JL, McVeigh ER. In vivo measurement of T*2 and field inhomogeneity maps in the human heart at 1.5 T. Magnetic resonance in medicine. 1998; 39:988–98. [PubMed: 9621923]
24. Storey PLW, Chen Q, Edelman RR. Dark flow artifacts with steady-state free precession cine MR technique: causes and implications for cardiac MR imaging. Radiology. 2004:230.
25. Bieri O, Scheffler K. Fundamentals of balanced steady state free precession MRI. Journal of magnetic resonance imaging : JMRI. 2013; 38:10.
26. Wu Y, Yang F, Chung YC. Robust and fast SSFP for the evaluation of LV function at 3T. Journal of Cardiovascular Magnetic Resonance. 2013; 15:1. [PubMed: 23324167]
27. Fessler JA. Model-based image reconstruction for MRI. Ieee Signal Proc Mag. 2010:9.
28. Lustig M, Donoho D, Pauly JM. Sparse MRI: The application of compressed sensing for rapid MR imaging. Magnetic resonance in medicine. 2007; 58:1182–1195. [PubMed: 17969013]
29. Lustig M, Donoho DL, Santos JM, Pauly JM. Compressed sensing MRI. Ieee Signal Proc Mag. 2008; 25:72–82.
30. Otazo R, Kim D, Axel L, Sodickson DK. Combination of Compressed Sensing and Parallel Imaging for Highly Accelerated First-Pass Cardiac Perfusion MRI. Magnetic resonance in medicine. 2010; 64:767–776. [PubMed: 20535813]
31. Schar M, Kozerke S, Fischer SE, Boesiger P. Cardiac SSFP imaging at 3 Tesla. Magnetic resonance in medicine. 2004; 51:799–806. [PubMed: 15065254]
32. Martin V, Drochon A, Fokapu O, Gerbeau JF. MagnetoHemoDynamics in the aorta and electrocardiograms. Phys Med Biol. 2012; 57:18.
33. Deshpande VS, Shea SM, Li D. Artifact reduction in true-FISP imaging of the coronary arteries by adjusting imaging frequency. Magnetic resonance in medicine. 2003; 49:803–9. [PubMed: 12704761]

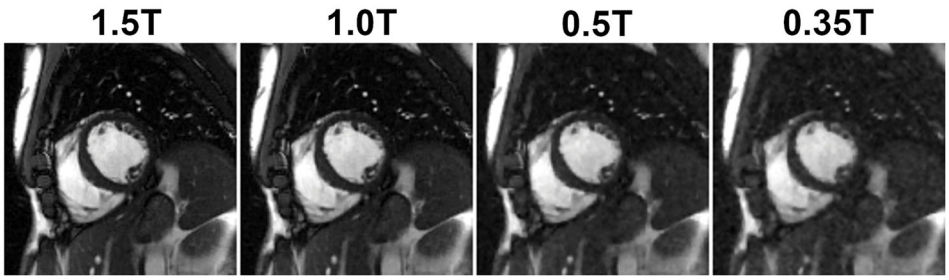

Figure 1.

Impact of retrospectively lowering SNR on the image quality. A prospectively downsampled (R=3) segmented cine dataset was collected on a 1.5T scanner from a healthy volunteer. Acquisition parameters include: matrix size: 256×192; FOV: 380×285 mm^2; TE/TR: 1.47/2.9 ms; slice thickness 8 mm; flip angle: 82°; bandwidth: 714 Hz/pixel; temporal resolution 47 ms; sampling pattern: VISTA; bSSFP-based prospectively triggered segmented sequence. Complex Gaussian noise was then added to simulate data at 1T, 0.5T and 0.35T field strengths. The image recovery was performed using SCoRe.

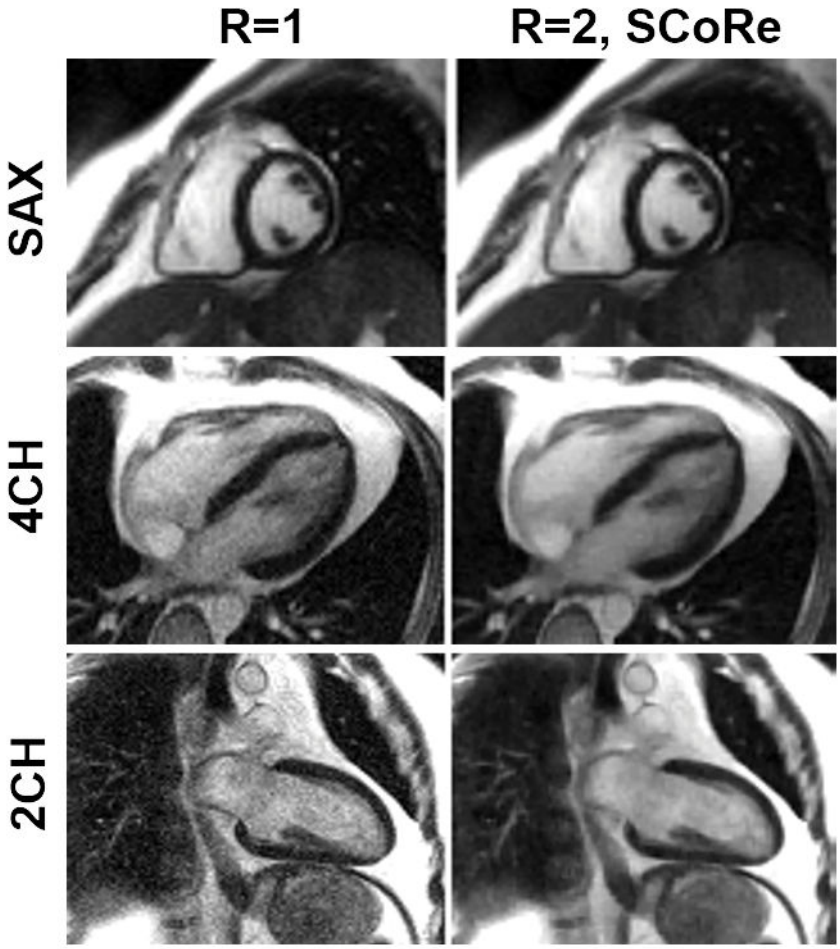

Figure 2.

Cine images from the data collected on a 0.35T scanner. Three fully sampled segmented cine datasets (with three different imaging orientations: short-axis (SAX), 4-chamber (4CH), and 2-chamber (2CH)) were collected using the following parameters. Matrix size: 160×120 (SAX), 160×120 (4CH), 192×180 (2CH); FOV: 400×400 mm^2 (SAX), 400×400 mm^2 (4CH), 400×360 mm^2 (2CH); TE/TR: 1.6/3.3 ms (SAX), TE/TR: 1.4/3.0 ms (4CH), TE/TR: 1.3/2.7 ms (SAX); slice thickness 8 mm; flip angle: 110°; bandwidth 558 Hz/pixel (SAX), bandwidth 789 Hz/pixel (4CH), bandwidth 1184 Hz/pixel (2CH), temporal resolution 40 ms (SAX), 45 ms (4CH), 40 ms (2CH); bSSFP-based prospectively triggered segmented sequence. For R=1, image recovery was based on the inverse Fourier transform of k-space data followed by sum-of-squares coil combine. For R=2, the data were retrospectively downsampled with VISTA, and the image recovery was based on SCoRe.

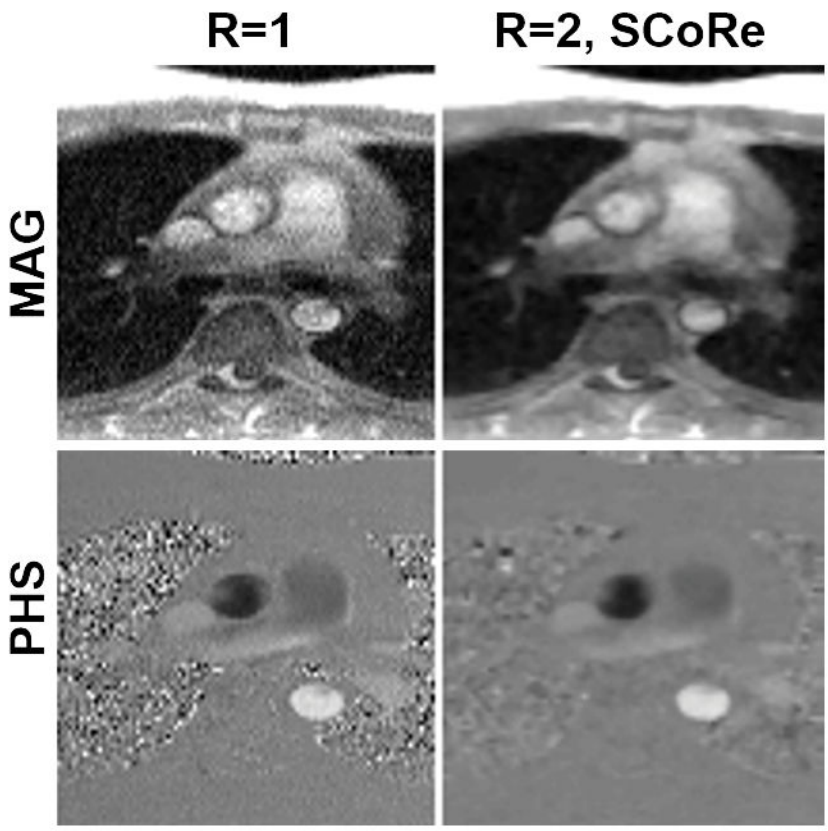

Figure 3.

Phase-contrast MRI images from the data collected on a 0.35T scanner. A fully sampled dataset was acquired using the following parameters. Matrix size: 192×108; FOV: 350×262 mm^2; TE/TR: 2.6/6.5 ms; slice thickness 8 mm; flip angle: 25°; bandwidth: 389 Hz/pixel; temporal resolution 52 ms; number of averages: 3; FLASH-based prospectively triggered segmented sequence. For R=1, image recovery was based on the inverse Fourier transform of k-space data followed by sum-of-squares coil combine. For R=2, the data were retrospectively downsampled with VISTA, and the image recovery was based on SCoRe. Note, for R=2, no averaging was employed.

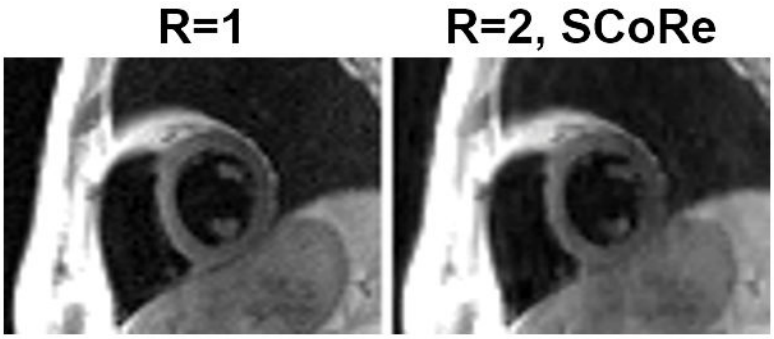

Figure 4.

Black blood images from the data collected on a 0.35T scanner. A fully sampled dataset was acquired using the following parameters. Matrix size: 192×114; FOV: 450×314 mm^2; TE: 40 ms; TR: two RR intervals; echo-train length: 19; echo spacing 6 ms; slice thickness 6 mm; bandwidth: 389 Hz/pixel; turbo spin echo-based segmented sequence. For R=1, image recovery was based on the inverse Fourier transform of k-space data followed by sum-of-squares coil combine. For R=2, the data were retrospectively downsampled with VISTA, and the image recovery was based on SCoRe.

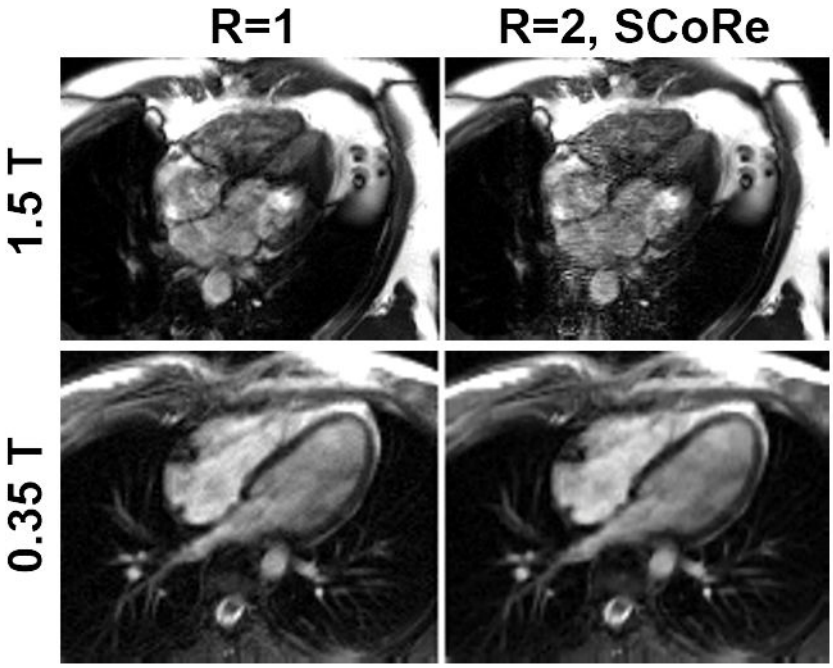

Figure 5.

Impact of long TR on image quality. Two fully sampled datasets—one on a 1.5T scanner (top row) and one on 0.35T scanner (bottom row)—were collected. For the dataset collected on 1.5T, the following parameters were used. Matrix size: 192×132; FOV: 450×314 mm^2; TE/TR: 4.6/9.2 ms; slice thickness 8 mm; flip angle: 110°; bandwidth: 134 Hz/pixel; temporal resolution 56 ms; bSSFP-based prospectively triggered segmented sequence. For the dataset collected on 0.35T, the following parameters were used. Matrix size: 192×126; FOV: 350×295 mm^2; TE/TR: 4.6/9.3 ms; slice thickness 8 mm; flip angle: 110°; bandwidth: 130 Hz/pixel; temporal resolution 56 ms; bSSFP-based prospectively triggered segmented sequence. For R=1, image recovery was based on the inverse Fourier transform of k-space data followed by sum-of-squares coil combine. For R=2, the data were retrospectively downsampled with VISTA, and the image recovery was based on SCoRe.